Bile-mediated ToxS homodimerization provides a model for ToxRS periplasmic interactions

Minje Kim[1], Deepak Balasubramanian[2], F. Jon Kull[1], Salvador Almagro-Moreno[2,3]*, Charles R. Midgett[1]*

[1]Department of Chemistry, Dartmouth College, Hanover, NH, USA

[2]Department of Host-Microbe Interactions, St. Jude Children's Research Hospital, Memphis, TN, USA

[3]St. Jude Children's Research Hospital Graduate School of Biomedical Sciences, St. Jude Children's Research Hospital, Memphis, TN, USA

*For correspondence: Charles R. Midgett; charles.r.midgett@dartmouth.edu (CRM), Salvador Almagro-Moreno; samoreno@stjude.org (SAM)

Running title: Bile mediates ToxS periplasmic domain homodimerization

ABSTRACT

The ToxRS system belongs to a family of co-component transmembrane transcription regulators that act as sensors of environmental cues and regulate virulence gene expression in several bacterial pathogens. These systems are thought to operate by sensing environmental stimuli and transmitting signals through periplasmic domains to activate DNA-binding transcription factors. In the enteric pathogens *Vibrio parahaemolyticus* and *Vibrio cholerae*, the ToxRS system regulates virulence factors responsible for severe gastrointestinal symptoms in humans. ToxR is a DNA-binding regulator associated in the periplasm with ToxS, a protein of poorly understood function. ToxS modulates the activity of its binding partner ToxR in the presence of bile salts, antimicrobial cholesterol metabolites secreted into the gut. To date, the molecular mechanism underlying this regulation remains unclear. We present crystal structures of the *V. parahaemolyticus* ToxS periplasmic domain (ToxSp) with and without the bile salt glycocholate. ToxSp forms an 8-stranded broken β-barrel with a central α-helix and is structurally homologous to a group of chaperone proteins. ToxSp has a highly conserved hydrophobic core that stabilizes the β-barrel fold, while the binding pocket tolerates substantial variation, consistent with binding hydrophobic ligands. Strikingly, we discovered that Vp-ToxSp binds three molecules of glycocholate and the presence of this bile salt leads to the formation a strand-swapped ToxS homodimer. Finally, modeling two ToxR periplasmic domains in complex with the glycocholate-bound ToxSp homodimer provides a structure-based model for bile salt-mediated heterotetramerization of the ToxRS system. Overall, our study addresses a major longstanding question in the field of Vibrio virulence regulation providing a scenario that could apply to other pathogens that utilize these membrane-bound family transcriptional regulators.

AUTHOR SUMMARY

The ability to sense the environment is essential for bacterial pathogens to successfully colonize the human host. Many pathogenic bacteria utilize members of the family of co-component transmembrane transcription regulators (coTTRs) to regulate pathogenesis in response to host signals. The ToxRS system is a coTTR regulatory pair that is essential for host colonization and virulence regulation of the enteric pathogens *Vibrio cholerae* and *Vibrio parahaemolyticus*. This system encompasses a transcription factor, ToxR, and a binding partner of enigmatic function, ToxS. Here, we solved the structure of the ToxS periplasmic domain *V. parahaemolyticus* and found that it belongs to a larger family of chaperone-like proteins present in many organisms. Strikingly, we discovered that the presence of the bile salt glycocholate leads to the dimerization of the periplasmic domain of ToxS. We propose that bile salt-induced ToxS dimerization brings two ToxR cognates together forming a heterotetramer activating the regulatory system. Our results and model address a major longstanding question in the fields of Vibrio virulence regulation and could apply to other pathogens that utilize these membrane bound family transcriptional regulators.

49 **INTRODUCTION**

50 Many pathogenic bacteria utilize the family of co-component transmembrane transcription regulators
51 (coTTRs) to regulate pathogenesis in response to host signals [1]. These include VtrAC and ToxRS in *Vibrio*
52 spp., PsaEF from *Yersinia* spp., GrvA-FidL from enterohemorrhagic *Escherichia coli*, and YqeIJ from avian
53 pathogenic *E. coli* [2–8]. CoTTRs consist of a transmembrane transcription factor with an N-terminal winged
54 helix-turn-helix DNA-binding domain, a transmembrane helix and a C-terminal periplasmic domain, together
55 with a periplasmic binding partner that has a short N-terminal tail, a transmembrane helix, and a C-terminal
56 periplasmic domain [1,9]. While the periplasmic domains of these proteins have little sequence homology
57 between family members, many are clearly structural homologs [7,10,11]. These two-protein systems form
58 obligate heterodimers where they modulate gene expression in response to host signals for survival and
59 colonization [1,12]. This is thought to occur by the binding partner sensing a stimulus, such as a small
60 molecule, and then transducing the signal to the transcription factor through their respective periplasmic
61 domains [7,12,13]. To date, the mechanistic link between signal sensing by the periplasmic binding partner
62 and DNA binding by the cognate transcription factor remains unknown.

63 The ToxRS coTTR system acts as an environmental sensor and is conserved across the
64 Vibrionaceae family, a diverse group of aquatic bacteria [14–16]. Importantly, in several pathogenic *Vibrio*
65 species, ToxRS also acts as a virulence regulator and confers resistance against antimicrobial insults found
66 in the GI tract such as bile salts, cholesterol metabolites produced in the liver and secreted into the intestine
67 [3,15,17,18]. In *Vibrio cholerae,* the etiological agent of cholera, ToxRS helps mediate the stress response
68 to bile salts by modulating the transcription of two outer membrane porins, OmpU and OmpT [19,20].
69 Furthermore, together with another coTTR pair, TcpPH, ToxRS activates the virulence cascade via the
70 transcription of the master virulence regulator *toxT* [21–23]. ToxT directly promotes the production of two
71 critical virulence factors: the cholera toxin and toxin co-regulated pilus, which are essential for disease
72 symptoms to occur [24–27]. Similarly, in *Vibrio parahaemolyticus*, a source of gastrointestinal illness, ToxRS
73 regulates bile responses and essential virulence genes [3,18]. Together with another coTTR system, VtrAC

74 and ToxRS promote the expression of *vtrB*, which activates transcription of genes encoding the type III
75 secretion system [3,28,29].

76 Numerous studies have demonstrated the role of ToxR in these processes. However, despite its
77 relevance and ubiquitousness, the specific role of ToxS has remained obscure for decades. Studies using
78 mouse models of *V. cholerae* and *V. parahaemolyticus* infection show that ToxS is essential for intestinal
79 colonization, with Δ*toxS* strains exhibiting severe colonization defects [3,30]. Our laboratories and others
80 have shown that ToxS stabilizes ToxR against premature intramembrane proteolysis by leading to a
81 conformation that induces the formation of an intra-chain disulfide bond [31–33]. Furthermore, ToxS is
82 required for full ToxR activity in response to several stimuli including bile salts [13,34,35]. In minimal media,
83 ToxR requires ToxS to respond to bile salts and the amino acid mixture NRES [36,37]. Overall, these data
84 suggest that ToxRS exhibits on and off states, with ToxS being central for this switch-like process [36,37].
85 To date, the molecular mechanisms that mediate ToxRS interactions and the specific role of ToxS in these
86 processes remain unknown. Here, we solved the structure of the apo and glycocholate-bound ToxS
87 periplasmic domain (ToxSp) from *V. parahaemolyticus* (Vp-ToxSp). ToxSp is monomeric in the apo state
88 and dimeric in the bile salt-bound state, suggesting ToxS directly senses environmental stress signals and
89 dimerizes upon ligand binding. Additionally, a structural analysis of ToxSp suggests it is related to a group
90 of chaperone proteins. Our results suggest that coTTRs oligomerization is directed by interactions of the
91 periplasmic binding partner with environmental stimuli, which leads to heterotetramer formation with the
92 cognate transcription factor.

93

94 **RESULTS**

95 **ToxS periplasmic domain adopts a broken β-barrel fold with a putative ligand-binding pocket.** The *V.*
96 *parahaemolyticus* ToxS periplasmic domain residues Ser25-Asn171 (Vp-ToxSp) was cloned into an *E. coli*
97 expression system and purified using chitin-based affinity purification. Diffraction quality apo ToxSp crystals
98 were obtained using a seeded crystallization method and resolved to 1.9 Å resolution (**Table S1**). The
99 resulting structure reveals the Vp-ToxSp domain adopts a monomeric eight-stranded broken β-barrel, with

100 two copies in the asymmetric unit. The domain begins with the N-terminal helix (α1), positioned at the base
101 of the β-barrel, proximal to the inner membrane, followed by five β-strands (β1-β5), a second α-helix (α2),
102 and three final β-strands (β6-β8), with several disordered loops connecting the β-strands. Barrel closure is
103 enabled by hydrogen-bonding interactions between β1 of the N-terminus and the C-terminal β-strands (β6-
104 β8). (**Figure 1A, 1B**).

105 The central core consists of alternating hydrophobic and hydrophilic regions and the membrane-distal
106 face contains a solvent-accessible ~745 $Å^3$ cavity that likely functions as a small molecule binding region
107 extending toward the membrane (**Figure 1C right**) [38]. It is characterized by hydrophobic residues forming
108 the upper rim, a ring of hydrophilic residues in the middle, and a deeper hydrophilic cavity sealed at its base
109 by α1 (**Figure 1C left**). Interestingly, the pocket architecture resembles those observed in previously
110 characterized bile-binding proteins, suggesting a similar ligand-recognition role for Vp-ToxSp [7,11,39].

111

112 **Core conservation and pocket variability in ToxS.** To examine the amino acid conservation across the
113 Vibrionaceae family, 280 ToxR sequences were aligned using Unipro UGENE, and the corresponding ToxS
114 sequences were arranged in the same order [40]. Both sets of sequences were analyzed using Clustal
115 Omega (EMBL) to generate percent identity matrices (**Figure S1, S2**) [41]. Comparison of these matrices
116 revealed two key trends: first the ToxS periplasmic domain (ToxSp) is more conserved than the ToxR
117 periplasmic domain and second the clustering patterns observed for ToxSp mirror those of ToxRp,
118 suggesting coordinated evolutionary pressures on both components of the ToxRS pair. To examine residue-
119 level conservation, the ToxSp alignment was analyzed in ChimeraX using AL2CO [42]. The most strongly
120 conserved residues localize to the hydrophobic core, with three residues, Trp37, Gly99, and Trp101, showing
121 100% conservation across all analyzed sequences (**Figure 1D and inset**). The two tryptophan residues are
122 packed deep within the hydrophobic core, while Gly99 appears to contribute to a kink in β4, influencing the
123 positioning of Trp101, highlighting the importance of this region in the overall structure. In contrast, residues
124 surrounding the ligand-binding pocket exhibit low sequence identity across Vibrionaceae (**Figure 1D**).
125 Despite this variability, many positions within the pocket retain a strong preference for hydrophobic side

126 chains, with several sites remaining >90% hydrophobic and others maintaining hydrophobicity in ~70% of
127 sequences (**Table S2**). Together, these observations indicate that ToxS is built upon a highly conserved
128 hydrophobic core that stabilizes the β-barrel fold, while the pocket tolerates substantial variation, consistent
129 with binding hydrophobic ligands through largely non-specific interactions. Finally, low conservation at the
130 ToxS-ToxR binding interface supports the idea that these two proteins have coevolved at their binding
131 interfaces.
132
133 **The ToxS periplasmic domain fold is related to a large group of chaperones.** Having defined the overall
134 structure of Vp-ToxSp, we next sought to determine whether this architecture resembles any previously
135 characterized protein families. Because structural homology can provide functional insights in the absence
136 of primary sequence conservation, we used DALI to identify proteins with related three-dimensional folds
137 (**Table S3**) [43]. This search revealed VtrC, its closest known homolog in *V. parahaemolyticus*, as the top hit,
138 validating the approach. Additional significant matches containing this fold were identified, including
139 periplasmic chaperones HslJ (PDB ID: 2KTS), first identified in *Escherichia coli* and MxiM from *Shigella*
140 *flexneri* [44–46]. Structural similarity was also observed with an AlphaFold-predicted structure of META1,
141 part of the META family in *Leishmania* spp. (**Figure 2A**), indicating that ToxS-like proteins are distributed in
142 a wide range of taxa [47]. Despite their evolutionary diversity, these proteins share topological features,
143 including the C-terminal β-strands (β6-β8) (green) and the central α-helix (orange) (**Figure 2B**).
144 The structural and topological relatedness between these proteins is mirrored by parallels in function,
145 as many of the identified hits serve as periplasmic chaperones and/or respond to stress. Consistent with this,
146 ToxS stabilizes the ToxR periplasmic domain and promotes disulfide bond formation [33,48]. Likewise, VtrC
147 in *V. parahaemolyticus* stabilizes VtrA to turn on the expression of *vtrB* that activates the type III secretion
148 system 2 [7]. HslJ functions as a stress-induced periplasmic chaperone in multiple bacterial species [46,49–
149 52] and MxiM acts as a pilot protein required for type III secretion system-mediated host cell invasion in
150 *Shigella* spp. [53]. Although the role of META1 is less clear, its overexpression increases virulence in mice
151 infected with *Leishmania amazonensis*, and the related META2 protein is upregulated in response to heat

shock and oxidative stress [47,52,54,55]. Despite these structural and functional similarities (**Figure 2A**), ToxS, HslJ, MxiM, and META1 display very limited sequence homology, suggesting strong evolutionary pressure to conserve fold and function rather than the primary sequence [47].

Vp-ToxSp bound to bile salts forms a strand-swapped dimer. The 1.9 Å crystal structure of Vp-ToxSp bound to glycocholate reveals a pronounced ligand-induced conformational change relative to the apo structure (**Figure 3A; Table S1**). Although each monomer retains the characteristic 8-stranded broken β-barrel fold with two α-helices, the bile salt-bound form assembles into a strand-swapped dimer in which β8 strands of the two monomers exchange positions (**Figure 3B**), with two dimers in the asymmetric unit. Notably, the swapped β8 strands align in the same register as in the apo state, preserving the hydrogen-bonding pattern of the β-barrel. In contrast to the apo structure, all loops at the top of the barrel are fully resolved, with the loop between β1 and β2 folding over the top of the barrel, capping the ligand-binding pocket. The orientation of the two N-termini within the dimer is compatible with the insertion of adjacent transmembrane helices into the membrane (see below).

Three glycocholate molecules stabilize the ToxSp dimer interface. The strand-swapped ToxSp dimer structure contains three glycocholate molecules bound between the two monomers toward the top of the β-barrel. In each monomer, glycocholate binds the hydrophobic pocket formed by residues from β1, β2, β3, and α2 (**Figure S3A**). The third glycocholate occupies a central site created by the juxtaposition of the C-terminal ends of two α2 helices from the two monomers, effectively bridging the two monomer-bound ligands. Across these sites, the glycocholates adopt a common orientation: their hydrophobic rings embed into the upper hydrophobic region of the binding pocket, while the polar hydroxyl and glycine groups remain solvent-exposed (**Figure 3C**). Although the interaction network is broadly conserved, the monomers contribute asymmetrically to ligand contacts at the interface. Two additional glycocholate molecules are present at the crystal-packing interfaces but display weaker electron density and are unlikely to be physiologically relevant (**Figure S3B**). The presence of an extended binding pocket in the ToxSp dimer that is absent in the apo

178 structure supports a model in which binding of three glycocholate molecules promotes ToxSp dimerization.
179 β8 strand swapping further stabilizes this conformation. These observations indicate that ToxS functions as
180 a ligand-responsive sensor that undergoes a monomer-to-dimer transition upon bile binding.
181
182 **ToxS and VtrC bind bile salts through distinct mechanisms.** Comparison of bile salt-bound structures of
183 ToxSp and VtrC demonstrates that, despite their shared broken β-barrel architecture, these proteins bind
184 bile salts in distinct ways. In VtrC, taurodeoxycholate and chenodeoxycholate occupy a pocket formed
185 directly within the β-barrel [7,39]. In ToxSp, however, helix α2 occupies the position taken up by bile salts in
186 VtrC, and the β1-β2 loop folds over the top of the barrel, an architectural feature that is absent in VtrC (**Figure**
187 **3D, 3E**). As a result, the orientation of glycocholate differs substantially: the side chain of glycocholate
188 projects outward, rather than upward, as observed in VtrC (**Figure 3F**). This outward orientation exposes the
189 hydrophilic tail of the glycine moiety to solvent, potentially allowing ToxSp to accommodate bile salts with
190 diverse side chains. These differences suggest that although ToxS and VtrC share an overall broken β-barrel
191 fold, the coTTR binding partners have evolved distinct ligand-binding strategies while preserving the
192 conserved broken β-barrel scaffold.
193
194 **ToxSp bound to bile adopts a conformation resembling the ToxR-bound state.** To determine whether
195 bile salt binding induces conformational changes relevant to ToxR engagement, we compared the apo and
196 glycocholate-bound *V. parahaemolyticus* ToxSp structures with the *V. cholerae* ToxSp (Vc-ToxSp) from the
197 heterodimeric ToxRS complex. This analysis reveals that bile salt binding drives Vp-ToxSp into a
198 conformation closely resembling the ToxR-bound state (**Figure 3G**) [11]. In the apo structure of Vp-ToxSp,
199 the β1 strand of the barrel is bent inward, with a single water molecule bridging β1 and β8, resulting in a
200 more closed conformation consistent with the absence of a ligand or binding partner (**Figure 3H**). In contrast,
201 the glycocholate-bound Vp-ToxSp structure adopts a more open architecture, with two waters occupying the
202 space between the β1 and β8 strands. This arrangement parallels the Vc-ToxSp-ToxRp complex, in which
203 Thr279 of ToxR occupies a position analogous to the two waters observed in glycocholate-bound Vp-ToxSp

204 (**Figure 3H**). These similarities suggest that bile salt binding primes ToxS for interaction with ToxR by
205 inducing a more open conformation of the β-barrel. This observation is also consistent with prior biochemical
206 evidence that bile salts and detergents such as Triton X-100 enhance ToxRp-ToxSp association [18].
207 Together, these structural and biochemical observations indicate that bile salt binding not only drives ToxS
208 dimerization but also prepares ToxS for a productive engagement with ToxR, thereby enabling ToxRS
209 complex formation.
210

211 **DISCUSSION**

212 In this study, we report the crystal structures of ToxSp in apo and glycocholate-bound forms and propose
213 that bile-binding induces dimerization of ToxS and formation of a ToxRS heterotetramer. While ToxS is
214 characterized as a member of the lipocalin protein family, analysis of the ToxSp topology and structure shows
215 that it closely resembles a group of chaperone proteins including HslJ (PDB ID: 2KTS), META1, and MxiM
216 [7,44,45,47,56]. Like ToxS, some of these proteins can stabilize their partner complexes and respond to
217 stress. HslJ is expressed and secreted into the periplasm under stress conditions [46,52]. MxiM acts as a
218 pilot protein for the type III secretion system in *Shigella* spp*.,* whereas META1 is thought to play a role in
219 secretion in *Leishmania* spp. [44,45,47]. These proteins share structure, topology, periplasmic localization of
220 the bacterial proteins, and chaperone-like features, which suggest that ToxS and other coTTRs are
221 evolutionarily related to a broader class of chaperone-like proteins with distinct cellular roles [12].

222 In addition to the topological analysis, the sequence conservation analysis of the ToxRS periplasmic
223 domains shows that ToxS is more conserved across species than ToxR. Nonetheless, our analyses support
224 the idea that the ToxRS system has co-evolved (**Figure S1, S2**). The most highly conserved ToxS residues
225 are located in the hydrophobic core, proximal to the membrane, suggesting that maintaining a stable, broken
226 β-barrel fold is crucial for ToxS function. In contrast, while the specific residues surrounding the ligand-binding
227 pocket vary, their hydrophobic and hydrophilic natures are preserved across the Vibrionaceae family (**Table**
228 **S2**). We contend that this allows the potential binding of various hydrophobic compounds, as demonstrated

229 by: ToxR being activated by several bile salts, as well as sodium dodecyl sulfate, and the interactions
230 between ToxRp and ToxSp increasing in the presence of Triton X-100 [18,37].
231 A key mechanistic question regarding the function of coTTR systems is how environmental signals activate
232 critical transcriptional responses at the molecular level. To date, it has been proposed that the periplasmic
233 domain of the ToxRS system senses environmental stimuli and transduces signals through the periplasmic
234 binding interface to the cytoplasmic DNA-binding domain [7,13]. Specifically, for both ToxRS and VtrAC, it
235 was thought that the ToxRS heterodimer potentially acted by binding to bile salts [7,11]. The structure of
236 GCH-bound ToxSp provides the first mechanistic evidence of a physical interaction of ToxS with host-stimuli
237 and shows ToxRS heterodimerization is not required for bile recognition. Given ligands and swapped strands
238 are absent in the monomeric apo form, bile salt binding appears to be the driving force for ToxS dimerization.
239 To investigate how bile-binding could locally cluster ToxR, we modeled the ToxR periplasmic domain
240 onto the GCH-ToxSp dimer structure. We aligned two copies of ToxRp from the *V. cholerae* heterodimeric
241 ToxRS periplasmic domain structure onto each chain in our GCH-ToxSp structure [11]. This alignment shows
242 that all four N-termini of the subunits appear to face the same direction and that both domain pairs are
243 positioned to be near the membrane. Furthermore, our predicted model indicates that there are minimal steric
244 clashes between ToxS and ToxR in the heterotetramer (**Figure 4**).
245 Based on the results presented here and the ToxRS model described above, we propose a
246 mechanism for which bile salts result in the dimerization of the ToxRS complex. First, monomeric ToxS on
247 the membrane binds bile salts, inducing dimerization as well as a conformational change in the β-barrel,
248 opening the space between β1 and β8, making it easier for ToxR to bind ToxS (**Figure 4, path C-D**).
249 Alternatively, if ToxS and ToxR can form a heterodimer in the absence of bile salts, we propose that bile salt
250 binding to ToxS will subsequently induce formation of the ToxRS heterotetramer (**Figure 4, path E-D**).
251 Overall, our model provides a scenario that suggests how bile salts may function as molecular signals that
252 pair periplasmic sensing to activation of the ToxRS system. More generally, we propose the binding partner
253 proteins of coTTR systems have evolved as chaperones that stabilize their cognate transcription factors and
254 serve as binding partners mediating dimerization.

255

256 **MATERIALS AND METHODS**

257 **Cloning of *V. parahaemolyticus* ToxS periplasmic domain**. The DNA sequence of the *V.*
258 *parahaemolyticus* ToxS periplasmic domain (residues S24-N171) [WP_020840240] was codon-optimized
259 and synthesized to include a SapI site, the coding sequence, and a BamHI site, flanked by primer binding
260 sites. The fragment was amplified with PCR, digested with SapI and BamHI restriction enzymes, and purified
261 using the PCR purification kit (Qiagen). The pTYB21 vector (NEB), containing an N-terminal chitin-binding
262 domain intein (CBD-intein) affinity tag, was digested with the same restriction enzymes (SapI and BamHI),
263 treated with calf intestinal phosphatase (CIP; NEB), and purified using the PCR purification kit (Qiagen)
264 (**Table S6**). The ToxSp insert was ligated into the prepared pTYB21 vector using Quick Ligase (NEB), and
265 the ligation products were transformed into *E. coli* DH5α cells (NEB). The transformants were selected on an
266 LB agar plate containing 100 µg/mL carbenicillin and screened by colony PCR for the correct insert size. The
267 selected colonies were grown in small-scale cultures; a portion was stored at -80 °C, while plasmid DNA
268 from the remaining culture was purified using the Miniprep kit (Qiagen). Plasmid sequences were confirmed
269 by Sanger sequencing with primers complementary to the T7 promoter.

270

271 **Protein Expression and Purification**. The confirmed CBD-ToxSp plasmid was transformed into *E. coli*
272 BL21-CodonPlus (DE3) competent cells (Agilent Technologies). The starter culture was grown overnight at
273 30 °C in ZYP-0.8G medium supplemented with 200 µg/mL carbenicillin and 25 µg/mL chloramphenicol in a
274 shaking incubator [57]. The culture was used to inoculate Terrific Broth Modified media (Fisher Scientific) at
275 a 1:250 ratio, supplemented with 2 mM $MgSO_4$, 200 µg/mL carbenicillin, and 25 µg/mL chloramphenicol. The
276 cells were grown at 37 °C to an OD_{600} of 2-3, induced with 1 mM IPTG, and incubated at 18 °C for 16-20
277 hours. The cells were harvested by centrifugation at 4,500 × *g* for 25 minutes at 4 °C and resuspended in
278 lysis buffer (20 mM Tris-HCl pH 8.0, 200 mM NaCl, 1 mM EDTA) containing cOmplete protease inhibitor
279 cocktail tablets (Roche). Lysis was performed by passing the cells through a French press three times, and
280 the lysate was centrifuged at 100,000 × *g* for 45 minutes at 4 °C. The supernatant was filtered through a 0.45

281 μm filter before purification. The supernatant was passed over chitin-binding resin (NEB) pre-equilibrated
282 with Tris wash buffer (20 mM Tris-HCl pH 8.0, 200 mM NaCl) to capture the CBD-ToxSp fusion protein. The
283 resin was washed sequentially with 10 column volumes (CV) of high-salt Tris wash buffer (20 mM Tris-HCl
284 pH 8.0, 1 M NaCl) and 20 CV of Tris wash buffer. The resin was rapidly washed with 3 CV of Tris cleavage
285 buffer (20 mM Tris-HCl pH 8.0, 200 mM NaCl, 50 mM DTT, 0.5 mM PMSF, 1 mM EDTA, cOmplete protease
286 cocktail tablet) to saturate the resin and initiate on-column intein-mediated cleavage of the CBD tag. The
287 column was incubated at 23 °C for 16-40 hours. Cleaved ToxSp protein was eluted in Tris wash buffer,
288 concentrated using Amicon Ultra 3 kDa molecular weight cut-off (MWCO) centrifugal filters (Millipore), and
289 further purified by size-exclusion column (HiLoad 16/600 Superdex 200 pg, Cytiva) pre-equilibrated with gel
290 filtration buffer (20 mM Tris-HCl pH 8.0, 200 mM NaCl). The purified ToxSp protein solution was concentrated
291 to 9-16 mg/mL, flash-frozen in liquid nitrogen, and stored at -80 °C until crystallization.
292
293 **Crystallization and Data Collection**. To obtain apo ToxSp crystals, a seeded crystallization method was
294 used to promote the growth of diffraction-quality crystals. First, purified ToxSp protein was concentrated to
295 16 mg/mL and used to generate initial crystals. These initial ToxSp crystals were grown by combining protein
296 and crystallization solution (100 mM succinic acid pH 6.0, 16% (w/v) PEG 3,350) at a 1:1 ratio in a 96-well,
297 2-drop MRC plate (Swissci) with NT8 Drop Setter (Formulatrix). The resulting crystals were harvested and
298 stored in 50 μL crystallization solution, then disrupted with a polytetrafluoroethylene seed bead (Hampton
299 Research) to generate a seed stock. This stock solution was serially diluted (1:10 to 1:10,000) and stored at
300 room temperature (23 °C). For seeded crystallization, purified ToxSp protein was concentrated to 14 mg/mL
301 and seeded by adding the diluted seed stock at a 25:2 (v/v) protein-to-seed ratio. The crystallization trials
302 were set up in the 96-well, 2-drop MRC plates (Swissci) using the NT8 Drop Setter (Formulatrix) with protein-
303 to-reservoir ratios of 1:1 (drop 1) and 1:2 (drop 2), using 96-well sparse matrix crystal screens. Under these
304 conditions, the optimal diffraction-quality apo crystals were obtained from Berkeley crystal screen condition
305 E8 (Rigaku Reagents; 100 mM HEPES pH 7.5, 200 mM sodium malonate dibasic pH 7.0, 20% (w/v) PEG
306 monomethyl ether 2,000). The crystals were cryoprotected with a solution formulated with 70% crystal

307 reservoir solution and 30% glycerol. The diffraction data were collected at the NSLS-II AMX beamline
308 (Brookhaven National Laboratory) and processed to 2.1 Å resolution with XDS, yielding a space group of P
309 2_1 2_1 2_1 with unit cell parameters 53.746 58.230 89.456 90.000 90.000 90.000 (**Table S1**) [58].
310 To obtain glycocholate-bound ToxSp crystals, the frozen ToxSp protein stock at 16 mg/mL was
311 thawed and supplemented with 10 mM sodium glycocholate stock prepared in ToxSp buffer (20 mM Tris-
312 HCl pH 8.0, 200 mM NaCl) to achieve final concentrations of approximately 622 μM ToxSp and 3.13 mM
313 sodium glycocholate (1:5 protein-to-ligand ratio). The combined glycocholate-ToxSp solution was incubated
314 overnight at 4 °C with rotation to allow complex formation. The crystallization plates for the glycocholate-
315 bound complex were set up using the same seeding method as for apo ToxSp. The glycocholate-ToxSp
316 solution was seeded by adding diluted seed stock prepared from apo ToxSp crystals at a 25:2 (v/v) protein-
317 to-seed ratio. The crystallization trials were set up in 96-well, 2-drop MRC plates (Swissci) using 96-well
318 sparse matrix crystal screens. The initial crystal hit was observed from Index crystal screen condition H9
319 (Hampton Research). The Index H9 condition was optimized to 0.06 M zinc acetate dihydrate and 17% (w/v)
320 PEG 3,350. The crystals were cryoprotected with a solution formulated with 70% crystal reservoir solution
321 and 30% glycerol. The diffraction data were processed to 1.9 Å resolution with autoPROC, yielding a space
322 group of P 2_1 2_1 2_1 and a unit cell of 69.828 92.503 95.805 90.00 90.00 90.00 (**Table S1**) [59].
323
324 **Structure Determination**. The structure of apo ToxSp was determined by molecular replacement using an
325 AlphaFold structure prediction model, truncated to exclude regions with pLDDT under 90 [60]. The molecular
326 replacement was performed using Phaser [61]. The iterative refinement cycles were performed in Refine
327 from PHENIX, and manual model building was performed in COOT [62]. Structural visualization and analysis
328 were performed in ChimeraX [63]. The final structure was deposited in the Protein Data Bank (PDB ID: 8U2F).
329 The strand-swapped dimer structure of GCH-bound ToxSp was solved by molecular replacement using a
330 RoseTTAFold All-Atom prediction model generated as a monomer [64]. The electron density map clearly
331 indicated a strand swap in the β8 region, confirmed by a composite omit map in PHENIX [65]. The protein

332 structure and GCH ligands were built using COOT with ligand restraints from the REFMAC library [62,66].
333 The final structure visualization and analysis were performed in ChimeraX [63].
334
335 **Conservation analysis**. To analyze the ToxSp sequence conservation, BLAST was used to find sequences
336 homologous to the *V. cholerae* ToxR periplasmic domain residues 199-294 [67,68]. The resulting BLAST
337 sequences were then curated by removing entries that were multispecies alignments, partial sequences,
338 identical sequences, or sequences from the same species that were highly similar, leaving a list of ToxR
339 periplasmic domains primarily representing a single sequence per species. The curated ToxRp sequences
340 were aligned using MUSCLE and then used to generate a percent identity matrix with Clustal Omega
341 [41,69,70]. Based on this ToxRp sequence alignment, the corresponding ToxSp sequences from the same
342 species were identified in the NCBI and compiled into the same order as the aligned ToxRp sequences to
343 preserve one-to-one pairing [68]. This procedure resulted in a list of 280 paired ToxR and ToxS sequences.
344 The ToxS sequences were then aligned, and the sequences of the N-terminal tail and transmembrane
345 domain were removed so that only periplasmic domains (ToxSp) were retained. Both the ToxRp and ToxSp
346 sequences were subsequently aligned again, and a percent identity matrix calculated by Clustal Omega
347 without rearrangement of the sequence order [69]. Once the alignment was complete, the file with the ToxSp
348 alignment was loaded into ChimeraX to calculate and visualize the protein conservation at the residue level
349 using the built-in program AL2CO [42].
350
351 **ADDITIONAL INFORMATION**
352 Atomic coordinates and structure factors for the reported structures have been deposited in the Protein Data
353 Bank (PDB) under accession numbers 8U2F (apo Vp-ToxSp) and 9ZJO (GCH-bound Vp-ToxSp). The data
354 collection statistics are shown in Table S1 in supplementary information.
355
356 **ACKNOWLEDGEMENTS**

This work was supported by National Institute of Allergy and Infectious Diseases (NIAID) R01AI168157 and R21AI140740 to JFK. In addition, this work was also supported by a National Science Foundation (NSF) CAREER award (#2045671), a Burroughs Wellcome Investigator in the Pathogenesis of Infectious Disease (#1021977) and ALSAC at St. Jude Children's Research Hospital to SAM.

FIGURE LEGENDS

Figure 1. Structure and conservation of the *Vibrio parahaemolyticus* ToxS periplasmic domain. (A, B) Apo ToxSp from *V. parahaemolyticus* contains an 8-stranded broken beta-barrel fold and the central alpha-helix (β-strands; dark-blue, α-helices; light blue, coils; gray). (C) Left panel: apo ToxSp has a binding pocket (left panel, pink) enclosed by the β-barrel and the central helix (grey). Right panel: the binding pocket constitutes a central region of hydrophilic residues (blue) flanked by regions with hydrophobic (gold) residues. (D) Apo-Vp ToxSp structure colored based on conservation data obtained from sequence alignment across 280 Vibrionaceae family members reveals that only residues Trp37, Gly99, and Trp101 are 100% conserved.

Figure 2. ToxSp is a stress-responsive periplasmic chaperone. (A) Structural comparison of ToxSp with VtrC (PDB ID: 5KEV), HslJ (PDB ID: 2KTS), MxiM (PDB ID: 1Y9L), and META1 (AlphaFold: A0A088S6F1) highlights a shared broken β-barrel fold common among chaperone proteins. (B) The structural and topological similarities are highlighted by the C-terminal β-strands (β6-β8) (green) and the central α-helix (orange). (C) Under each topology are relevant highlights of the protein localization, function, and relevant binding partner.

Figure 3. Bile salt binding drives strand swapping and homodimerization of ToxS. (A) The GCH bound ToxSp dimer crystal structure shows two β8 strand swapped ToxSp monomers (blue and purple β-barrels) enclosing three glycocholate molecules (blue, orange, and pink). (B) Electron density map of the crystal structure surrounding the strand-swapped β8 loops (Ser160-Thr166) displayed as green mesh, contoured at 1σ. (C) Electron density map of the three glycocholate molecules bound to the ToxSp dimer displayed as

383 green mesh, contoured at 1σ. Comparison of (D) Vp-ToxSp-GCH with the protein in gray and the ligand in
384 blue, and (E) VtrC-taurodeoxycholate (PDB ID: 5KEW) with the protein in blue and the ligand in green,
385 complexes demonstrates the different binding orientations of the two ligands. (F) Overlay of the crystal
386 structures of GCH-bound Vp-ToxSp monomer, and taurodeoxycholate bound to VtrC (protein not shown for
387 clarity) highlights the differences in the ligand orientation. (G) Overlay of the apo Vp-ToxSp, (blue), and a
388 GCH-Vp-ToxSp monomer (cyan), and the Vc-ToxSp from the heterodimeric ToxRp-ToxSp complex (orange;
389 PDB: 8ALO). The comparison (inset) shows that apo Vp-ToxSp (blue) adopts a more closed conformation,
390 whereas both glycocholate-bound Vp-ToxSp (cyan) and Vc-ToxSp (orange) from the heterodimer with ToxR
391 display a more open conformation. (H) In apo Vp-ToxSp (blue, left), a single water molecule (red) bridges β1
392 and β8 strands to stabilize the closed conformation. In GCH-bound Vp-ToxSp (cyan, middle), two water
393 molecules (red) bind the more open interface, whereas in Vc-ToxSp (orange, right), Thr279 from Vc-ToxRp
394 (grey) plays the role of the water molecules, stabilizing the closed conformation.
395
396 **Figure 4. Model of the ToxRS heterotetramer in the inner membrane.** (A) Three molecules of
397 glycocholate (GCH, blue) bind to two Vp-ToxSp monomers (blue and purple β-barrels), promoting formation
398 of a ligand-bound homodimer, anchored in the inner membrane. (B) The ToxRp-ToxSp heterotetramer
399 model was generated using (ChimeraX) by positioning two chains of *Vibrio cholerae* ToxRp (PDB: 8ALO)
400 onto the glycocholate-bound Vp-ToxSp dimer. The arrangement places the periplasmic domains of ToxR
401 and ToxS in a physiologically plausible orientation with all four N-termini facing the inner membrane and
402 minimal steric interference between ToxR and ToxS (inset). (C-E) Model of the bile-mediated ToxRS
403 heterotetramer formation. Bile salts activate ToxRS through two possible pathways. In the first, (C) binding
404 of three GCH molecules to monomeric apo ToxS induces formation of a domain-swapped ToxS homodimer,
405 stabilizing an open β-barrel conformation that (D) enables ToxR recruitment and assembly of the active
406 heterotetramer. In the second pathway, (E) bile salts engage a pre-existing apo ToxRS heterodimer,
407 triggering conformational changes similar to those in ligand-bound ToxS that promote tetramerization of the
408 complex. Both mechanisms converge on formation of a bile-stabilized ToxRS heterotetramer (D).

REFERENCES

1. Demey LM, Gumerov VM, Xing J, Zhulin IB, DiRita VJ. Transmembrane transcription regulators are widespread in bacteria and archaea. Microbiol Spectr. 2023;11: 1–13. doi:10.1128/spectrum.00266-23
2. Herrington DA, Hall RH, Losonsky G, Mekalanos JJ, Taylor RK, Levine MM. Toxin, toxin-coregulated pili, and the *toxR* regulon are essential for *Vibrio cholerae* pathogenesis in humans. J Exp Med. 1988;168: 1487–1492. doi:10.1084/JEM.168.4.1487
3. Hubbard TP, Chao MC, Abel S, Blondel CJ, Wiesch PA Zur, Zhou X, et al. Genetic analysis of *Vibrio parahaemolyticus* intestinal colonization. Proc Natl Acad Sci U S A. 2016;113: 6283–6288. doi:10.1073/PNAS.1601718113/
4. Miller KA, Sofia MK, Weaver JWA, Seward CH, Dziejman M. Regulation by ToxR-like proteins converges on *vttRB* expression to control type 3 secretion system-dependent Caco2-BBE cytotoxicity in *Vibrio cholerae*. J Bacteriol. 2016;198: 1675. doi:10.1128/JB.00130-16
5. Quinn JD, Weening EH, Miner TA, Miller VL. Temperature control of *psaA* expression by PsaE and PsaF in *Yersinia pestis*. J Bacteriol. 2019;201. doi:10.1128/JB.00217-19
6. Morgan JK, Carroll RK, Harro CM, Vendura KW, Shaw LN, Riordan JT. Global regulator of Virulence A (GrvA) coordinates expression of discrete pathogenic mechanisms in enterohemorrhagic *Escherichia coli* through interactions with GadW-GadE. J Bacteriol. 2015;198: 394–409. doi:10.1128/JB.00556-15
7. Li P, Rivera-Cancel G, Kinch LN, Salomon D, Tomchick DR, Grishin N V., et al. Bile salt receptor complex activates a pathogenic type III secretion system. eLife. 2016;5. doi:10.7554/eLife.15718
8. Xue M, Xiao Y, Fu D, Raheem MA, Shao Y, Song X, et al. Transcriptional regulator YqeI, locating at ETT2 locus, affects the pathogenicity of avian pathogenic *Escherichia coli*. Animals (Basel). 2020;10: 1658. doi:10.3390/ANI10091658
9. Canals A, Pieretti S, Muriel-Masanes M, El Yaman N, Plecha SC, Thomson JJ, et al. ToxR activates the *Vibrio cholerae* virulence genes by tethering DNA to the membrane through versatile binding to multiple sites. Proc Natl Acad Sci U S A. 2023;120: e2304378120. doi:10.1073/PNAS.2304378120/
10. Midgett CR, Swindell RA, Pellegrini M, Kull FJ. A disulfide constrains the ToxR periplasmic domain structure, altering its interactions with ToxS and bile-salts. Scientific Reports. 2020;10: 1–11. doi:10.1038/s41598-020-66050-5
11. Gubensäk N, Sagmeister T, Buhlheller C, Geronimo BD, Wagner GE, Petrowitsch L, et al. *Vibrio cholerae*'s ToxRS bile sensing system. eLife. 2023;12. doi:10.7554/ELIFE.88721
12. Kinch LN, Cong Q, Jaishankar J, Orth K. Co-component signal transduction systems: fast-evolving virulence regulation cassettes discovered in enteric bacteria. Proc Natl Acad Sci U S A. 2022;119. doi:10.1073/pnas.2203176119
13. DiRita VJ, Mekalanos JJ. Periplasmic interaction between two membrane regulatory proteins, ToxR and ToxS, results in signal transduction and transcriptional activation. Cell. 1991;64: 29–37. doi:10.1016/0092-8674(91)90206-E
14. Reich KA, Schoolnik GK. The light organ symbiont *Vibrio fischeri* possesses a homolog of the *Vibrio cholerae* transmembrane transcriptional activator ToxR. J Bacteriol. 1994;176: 3085–3088. doi:10.1128/JB.176.10.3085-3088.1994

15. Lee SE, Shin SH, Kim SY, Kim YR, Shin DH, Chung SS, et al. *Vibrio vulnificus* has the transmembrane transcription activator ToxRS stimulating the expression of the hemolysin gene *vvhA*. J Bacteriol. 2000;182: 3405–3415. doi:10.1128/JB.182.12.3405-3415.2000/ASSET/78A3FD66-4658-4DDA-BD0D-385729E23392/
16. Welch TJ, Bartlett DH. Identification of a regulatory protein required for pressure-responsive gene expression in the deep-sea bacterium *Photobacterium* species strain SS9. Mol Microbiol. 1998;27: 977–985. doi:10.1046/J.1365-2958.1998.00742.X
17. Miller VL, Mekalanos JJ. Synthesis of cholera toxin is positively regulated at the transcriptional level by *toxR*. Proc Natl Acad Sci U S A. 1984;81: 3471–3475. doi:10.1073/PNAS.81.11.3471
18. Provenzano D, Schuhmacher DA, Barker JL, Klose KE. The virulence regulatory protein ToxR mediates enhanced bile resistance in *Vibrio cholerae* and other pathogenic *Vibrio* species. Infect Immun. 2000;68: 1491–1497. doi:10.1128/IAI.68.3.1491-1497.2000
19. Li CC, Crawford JA, DiRita VJ, Kaper JB. Molecular cloning and transcriptional regulation of *ompT*, a ToxR-repressed gene in *Vibrio cholerae*. Mol Microbiol. 2000;35: 189–203. doi:10.1046/J.1365-2958.2000.01699.X
20. Crawford JA, Kaper JB, DiRita VJ. Analysis of ToxR-dependent transcription activation of *ompU*, the gene encoding a major envelope protein in *Vibrio cholerae*. Mol Microbiol. 1998;29: 235–246. doi:10.1046/J.1365-2958.1998.00925.X
21. Morgan SJ, Felek S, Gadwal S, Koropatkin NM, Perry JW, Bryson AB, et al. The two faces of ToxR: activator of *ompU*, co-regulator of *toxT* in *Vibrio cholerae*. Mol Microbiol. 2011;81: 113–128. doi:10.1111/J.1365-2958.2011.07681.X
22. Crawford JA, Krukonis ES, DiRita VJ. Membrane localization of the ToxR winged-helix domain is required for TcpP-mediated virulence gene activation in *Vibrio cholerae*. Mol Microbiol. 2003;47: 1459–1473. doi:10.1046/J.1365-2958.2003.03398.X
23. Beck NA, Krukonis ES, DiRita VJ. TcpH influences virulence gene expression in *Vibrio cholerae* by inhibiting degradation of the transcription activator TcpP. J Bacteriol. 2004;186: 8309–8316. doi:10.1128/JB.186.24.8309-8316.2004
24. DiRita V, Parsot C, Jander G, Mekalanos J. Regulatory cascade controls virulence in *Vibrio cholerae*. Proc Natl Acad Sci U S A. 1991;88: 5403–5407. doi:10.1073/PNAS.88.12.5403
25. Higgins DE, DiRita VJ. Transcriptional control of *toxT*, a regulatory gene in the ToxR regulon of *Vibrio cholerae*. Mol Microbiol. 1994;14: 17–29. doi:10.1111/J.1365-2958.1994.TB01263.X
26. Krukonis ES, Yu RR, DiRita VJ. The *Vibrio cholerae* ToxR/TcpP/ToxT virulence cascade: distinct roles for two membrane-localized transcriptional activators on a single promoter. Mol Microbiol. 2000;38: 67–84. doi:10.1046/j.1365-2958.2000.02111.x
27. Withey JH, DiRita VJ. The toxbox: specific DNA sequence requirements for activation of *Vibrio cholerae* virulence genes by ToxT. Mol Microbiol. 2006;59: 1779–1789. doi:10.1111/J.1365-2958.2006.05053.X
28. Kaval KG, Chimalapati S, Siegel SD, Garcia N, Jaishankar J, Dalia AB, et al. Membrane-localized expression, production and assembly of *Vibrio parahaemolyticus* T3SS2 provides evidence for transertion. Nature Communications 2023 14:1. 2023;14: 1178-. doi:10.1038/s41467-023-36762-z
29. Rivera-Cancel G, Orth K. Biochemical basis for activation of virulence genes by bile salts in *Vibrio parahaemolyticus*. Gut Microbes. 2017;8: 366–373. doi:10.1080/19490976.2017.1287655

30. Pearson GDN, DiRita VJ, Goldberg MB, Boyko SA, Calderwood SB, Mekalanos JJ. New attenuated derivatives of *Vibrio cholerae*. Res Microbiol. 1990;141: 893–899. doi:10.1016/0923-2508(90)90127-C
31. Lembke M, Pennetzdorfer N, Tutz S, Koller M, Vorkapic D, Zhu J, et al. Proteolysis of ToxR is controlled by cysteine-thiol redox state and bile salts in *Vibrio cholerae*. Mol Microbiol. 2018;110: 796–810. doi:10.1111/MMI.14125
32. Almagro-Moreno S, Root MZ, Taylor RK. Role of ToxS in the proteolytic cascade of virulence regulator ToxR in *Vibrio cholerae*. Mol Microbiol. 2015;98: 963–976. doi:10.1111/mmi.13170
33. Ottemann KM, Mekalanos JJ. The ToxR protein of *Vibrio cholerae* forms homodimers and heterodimers. J Bacteriol. 1996;178: 156–162. doi:10.1128/JB.178.1.156-162.1996
34. Miller VL, DiRita VJ, Mekalanos JJ. Identification of *toxS*, a regulatory gene whose product enhances ToxR-mediated activation of the cholera toxin promoter. J Bacteriol. 1989;171: 1288–1293. doi:10.1128/jb.171.3.1288-1293.1989
35. Fengler VHI, Boritsch EC, Tutz S, Seper A, Ebner H, Roier S, et al. Disulfide bond formation and ToxR activity in *Vibrio cholerae*. PLoS One. 2012;7: 47756. doi:10.1371/journal.pone.0047756
36. Mey AR, Craig SA, Payne SM. Effects of amino acid supplementation on porin expression and ToxR levels in *Vibrio cholerae*. Infect Immun. 2012;80: 518–528. doi:10.1128/IAI.05851-11
37. Midgett CR, Almagro-Moreno S, Pellegrini M, Taylor RK, Skorupski K, Kull FJ. Bile salts and alkaline pH reciprocally modulate the interaction between the periplasmic domains of *Vibrio cholerae* ToxR and ToxS. Mol Microbiol. 2017;105: 258–272. doi:10.1111/mmi.13699
38. Volkamer A, Kuhn D, Rippmann F, Rarey M. DoGSiteScorer: a web server for automatic binding site prediction, analysis and druggability assessment. Bioinformatics. 2012;28: 2074–2075. doi:10.1093/bioinformatics/bts310
39. Zou AJ, Kinch L, Chimalapati S, Garcia N, Tomchick DR, Orth K. Molecular determinants for differential activation of the bile acid receptor from the pathogen *Vibrio parahaemolyticus*. J Biol Chem. 2023;299: 104591. doi:10.1016/J.JBC.2023.104591
40. Okonechnikov K, Golosova O, Fursov M, Varlamov A, Vaskin Y, Efremov I, et al. Unipro UGENE: a unified bioinformatics toolkit. Bioinformatics. 2012;28: 1166–1167. doi:10.1093/BIOINFORMATICS/BTS091
41. Sievers F, Wilm A, Dineen D, Gibson TJ, Karplus K, Li W, et al. Fast, scalable generation of high-quality protein multiple sequence alignments using Clustal Omega. Mol Syst Biol. 2011;7: 539. doi:10.1038/MSB.2011.75
42. Pei J, Grishin N V. AL2CO: calculation of positional conservation in a protein sequence alignment. Bioinformatics. 2001;17: 700–712. doi:10.1093/BIOINFORMATICS/17.8.700
43. Holm L, Laakso LM. Dali server update. Nucleic Acids Res. 2016;44: W351–W355. doi:10.1093/NAR/GKW357
44. Okon M, Moraes TF, Lario PI, Creagh AL, Haynes CA, Strynadka NCJ, et al. Structural characterization of the type-III pilot-secretin complex from *Shigella flexneri*. Structure. 2008;16: 1544–1554. doi:10.1016/j.str.2008.08.006
45. Lario PI, Pfuetzner RA, Frey EA, Creagh L, Haynes C, Maurelli AT, et al. Structure and biochemical analysis of a secretin pilot protein. EMBO J. 2005;24: 1111–1121. doi:10.1038/SJ.EMBOJ.7600610
46. Lilic M, Jovanovic M, Jovanovic G, Savic DJ. Identification of the CysB-regulated gene, *hslJ*, related to the *Escherichia coli* novobiocin resistance phenotype. FEMS Microbiol Lett. 2003;224: 239–246. doi:10.1016/S0378-1097(03)00441-5

537 47. Puri V, Goyal A, Sankaranarayanan R, Enright AJ, Vaidya T. Evolutionary and functional insights into
538 *Leishmania* META1: evidence for lateral gene transfer and a role for META1 in secretion. BMC Evol
539 Biol. 2011;11: 1–17. doi:10.1186/1471-2148-11-334/FIGURES/8
540 48. Pfau JD, Taylor RK. Mutations in *toxR* and *toxS* that separate transcriptional activation from DNA
541 binding at the cholera toxin gene promoter. J Bacteriol. 1998;180: 4724–4733.
542 doi:10.1128/JB.180.17.4724-4733.1998
543 49. Scribano D, Marzano V, Mortera SL, Sarshar M, Vernocchi P, Zagaglia C, et al. Insights into the
544 periplasmic proteins of *Acinetobacter baumannii* AB5075 and the impact of imipenem exposure: a
545 proteomic approach. Int J Mol Sci. 2019;20. doi:10.3390/IJMS20143451
546 50. Gao X, Zhang Z, Qian Q, Chen Q, Gu S, Li J, et al. Survival characteristics and transcriptomic analyses
547 reveal the adaptive response of the aquatic pathogen non-O1/O139 *Vibrio cholerae* to starvation
548 stress. Microbiol Spectr. 2022;10. doi:10.1128/SPECTRUM.01939-21
549 51. Fränzel B, Penkova M, Frese C, Metzler-Nolte N, Andreas Wolters D. *Escherichia coli* exhibits a
550 membrane-related response to a small arginine- and tryptophan-rich antimicrobial peptide. Proteomics.
551 2012;12: 2319–2330. doi:10.1002/PMIC.201100636
552 52. Scribano D, Pasqua M, Limongi D, Nencioni L, Palamara AT, Ambrosi C. The periplasmic protein HslJ
553 is the first-line of defense against oxidative stress in *Acinetobacter baumannii*. Biol Res. 2025;58: 2.
554 doi:10.1186/S40659-025-00584-8
555 53. Schuch R, Maurelli AT. The Mxi-Spa type III secretory pathway of *Shigella flexneri* requires an outer
556 membrane lipoprotein, MxiM, for invasin translocation. Infect Immun. 1999;67: 1982.
557 doi:10.1128/IAI.67.4.1982-1991.1999
558 54. Ramos CS, Yokoyama-Yasunaka JKU, Guerra-Giraldez C, Price HP, Mortara RA, Smith DF, et al.
559 *Leishmania amazonensis* META2 protein confers protection against heat shock and oxidative stress.
560 Exp Parasitol. 2011;127: 228–237. doi:10.1016/j.exppara.2010.08.004
561 55. Nourbakhsh F, Uliana SRB, Smith DF. Characterisation and expression of a stage-regulated gene of
562 *Leishmania* major. Mol Biochem Parasitol. 1996;76: 201–213. doi:10.1016/0166-6851(95)02559-6
563 56. Schaeffer RD, Medvedev KE, Andreeva A, Chuguransky SR, Pinto BL, Zhang J, et al. ECOD:
564 integrating classifications of protein domains from experimental and predicted structures. Nucleic
565 Acids Res. 2025;53: D411–D418. doi:10.1093/NAR/GKAE1029
566 57. Studier FW. Protein production by auto-induction in high density shaking cultures. Protein Expr Purif.
567 2005;41: 207–234. doi:10.1016/j.pep.2005.01.016
568 58. Kabsch W. XDS. Acta Crystallogr D Biol Crystallogr. 2010;66: 125. doi:10.1107/S0907444909047337
569 59. Vonrhein C, Flensburg C, Keller P, Sharff A, Smart O, Paciorek W, et al. Data processing and analysis
570 with the autoPROC toolbox. Acta Crystallogr D Biol Crystallogr. 2011;67: 293–302.
571 doi:10.1107/S0907444911007773
572 60. Jumper J, Evans R, Pritzel A, Green T, Figurnov M, Ronneberger O, et al. Highly accurate protein
573 structure prediction with AlphaFold. Nature. 2021;596: 583–589. doi:10.1038/S41586-021-03819-2
574 61. McCoy AJ, Grosse-Kunstleve RW, Adams PD, Winn MD, Storoni LC, Read RJ. Phaser
575 crystallographic software. J Appl Crystallogr. 2007;40: 658–674. doi:10.1107/S0021889807021206
576 62. Emsley P, Cowtan K. Coot: model-building tools for molecular graphics. Acta Crystallogr D Biol
577 Crystallogr. 2004;60: 2126–2132. doi:10.1107/S0907444904019158
578 63. Goddard TD, Huang CC, Meng EC, Pettersen EF, Couch GS, Morris JH, et al. UCSF ChimeraX:
579 Meeting modern challenges in visualization and analysis. Protein Sci. 2018;27: 14–25.
580 doi:10.1002/pro.3235

64. Krishna R, Wang J, Ahern W, Sturmfels P, Venkatesh P, Kalvet I, et al. Generalized biomolecular modeling and design with RoseTTAFold All-Atom. Science (1979). 2024;384. doi:10.1126/SCIENCE.ADL2528/
65. Adams PD, Afonine P V., Bunkóczi G, Chen VB, Davis IW, Echols N, et al. PHENIX: a comprehensive Python-based system for macromolecular structure solution. Acta Crystallogr D Biol Crystallogr. 2010;66: 213–221. doi:10.1107/S0907444909052925
66. Vagin AA, Steiner RA, Lebedev AA, Potterton L, McNicholas S, Long F, et al. REFMAC5 dictionary: organization of prior chemical knowledge and guidelines for its use. Acta Crystallogr D Biol Crystallogr. 2004;60: 2184–2195. doi:10.1107/S0907444904023510/
67. Altschul SF, Gish W, Miller W, Myers EW, Lipman DJ. Basic local alignment search tool. J Mol Biol. 1990;215: 403–410. doi:10.1016/S0022-2836(05)80360-2
68. Sayers EW, Beck J, Bolton EE, Brister JR, Chan J, Comeau DC, et al. Database resources of the National Center for Biotechnology Information. Nucleic Acids Res. 2024;52: D33–D43. doi:10.1093/NAR/GKAD1044
69. Madeira F, Madhusoodanan N, Lee J, Eusebi A, Niewielska A, Tivey ARN, et al. The EMBL-EBI Job Dispatcher sequence analysis tools framework in 2024. Nucleic Acids Res. 2024;52: W521–W525. doi:10.1093/NAR/GKAE241
70. Edgar RC. MUSCLE: multiple sequence alignment with high accuracy and high throughput. Nucleic Acids Res. 2004;32: 1792–1797. doi:10.1093/nar/gkh340

Figure 1

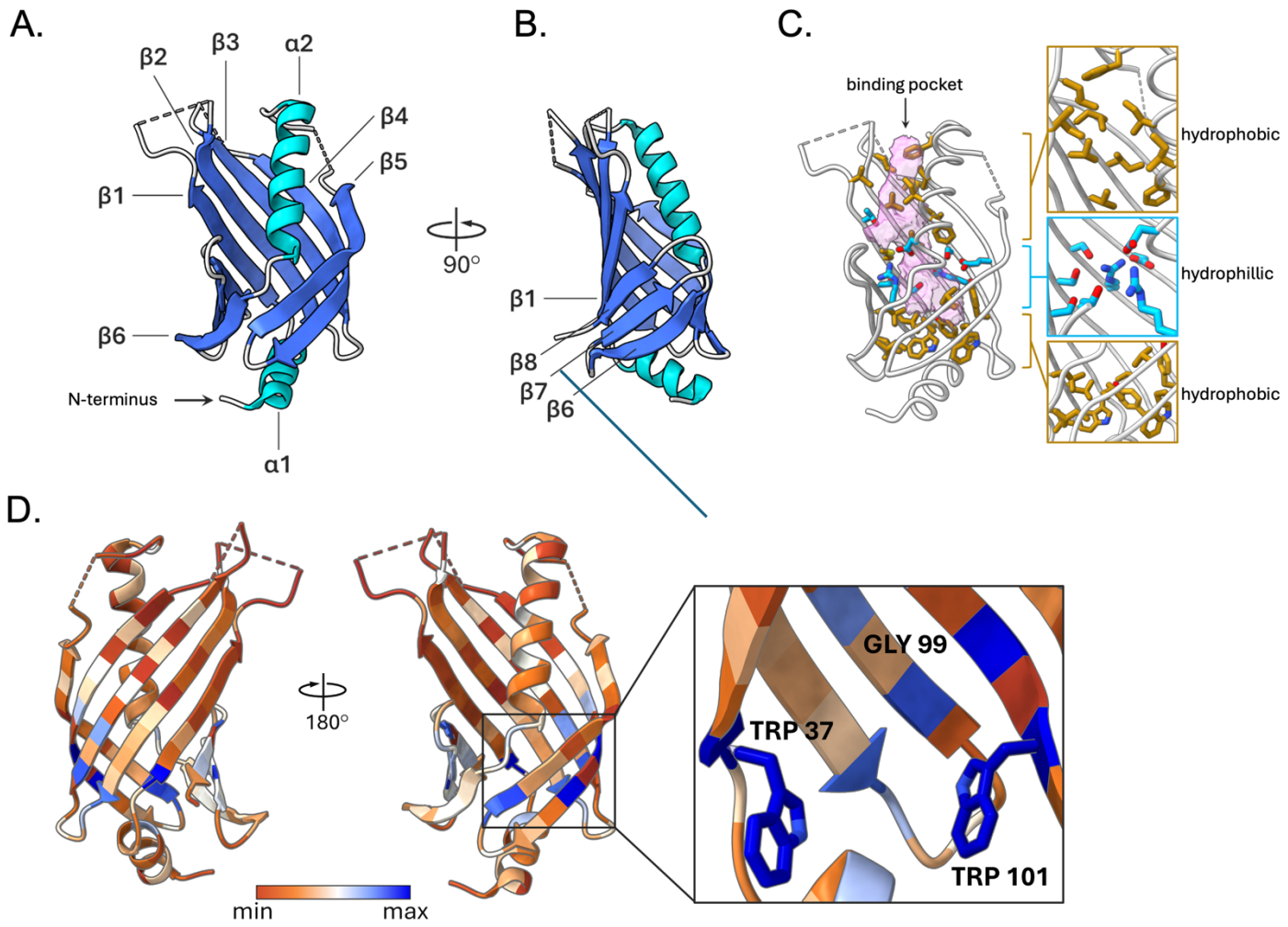
A.
β2
β3
α2
β4
β5
β1
β6
N-terminus
α1
90°
B.
β1
β8
β7
β6
C.
binding pocket
hydrophobic
hydrophillic
hydrophobic
D.
180°
min
max
GLY 99
TRP 37
TRP 101

602

Figure 2

A.

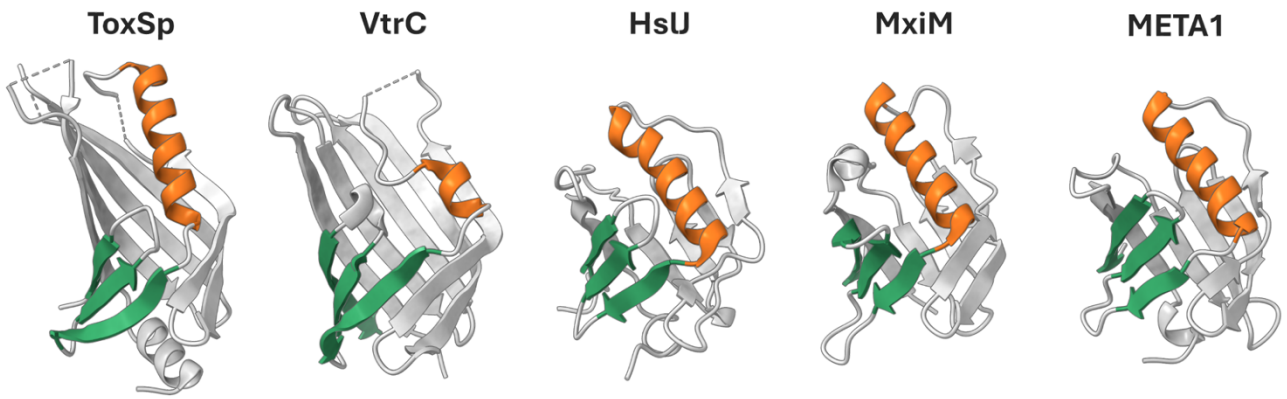

B.

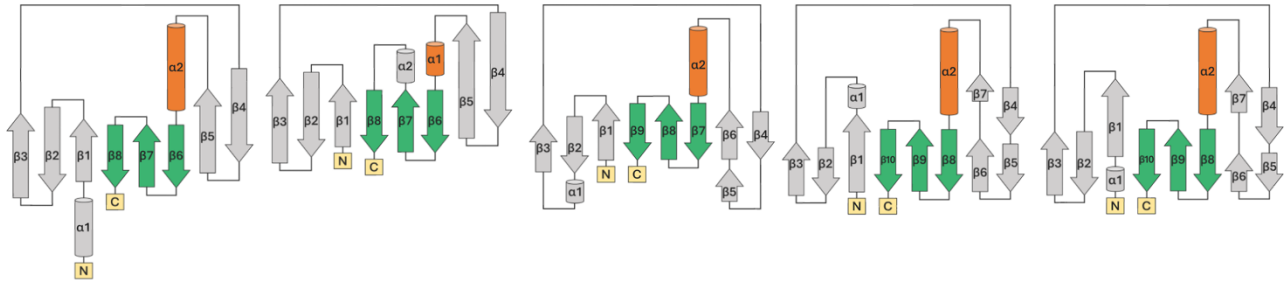

C.

	ToxS	VtrC	HsU	MxiM	META1
Domain localization	Periplasm	Periplasm	Periplasm	Periplasm	Flagellar pocket
Protein function	Membrane stress	T3SS expression	Stress response	Pilot protein	Secretory system(?)
Relevant partner	ToxR	VtrA		MxiD	

603
604
605

Figure 3

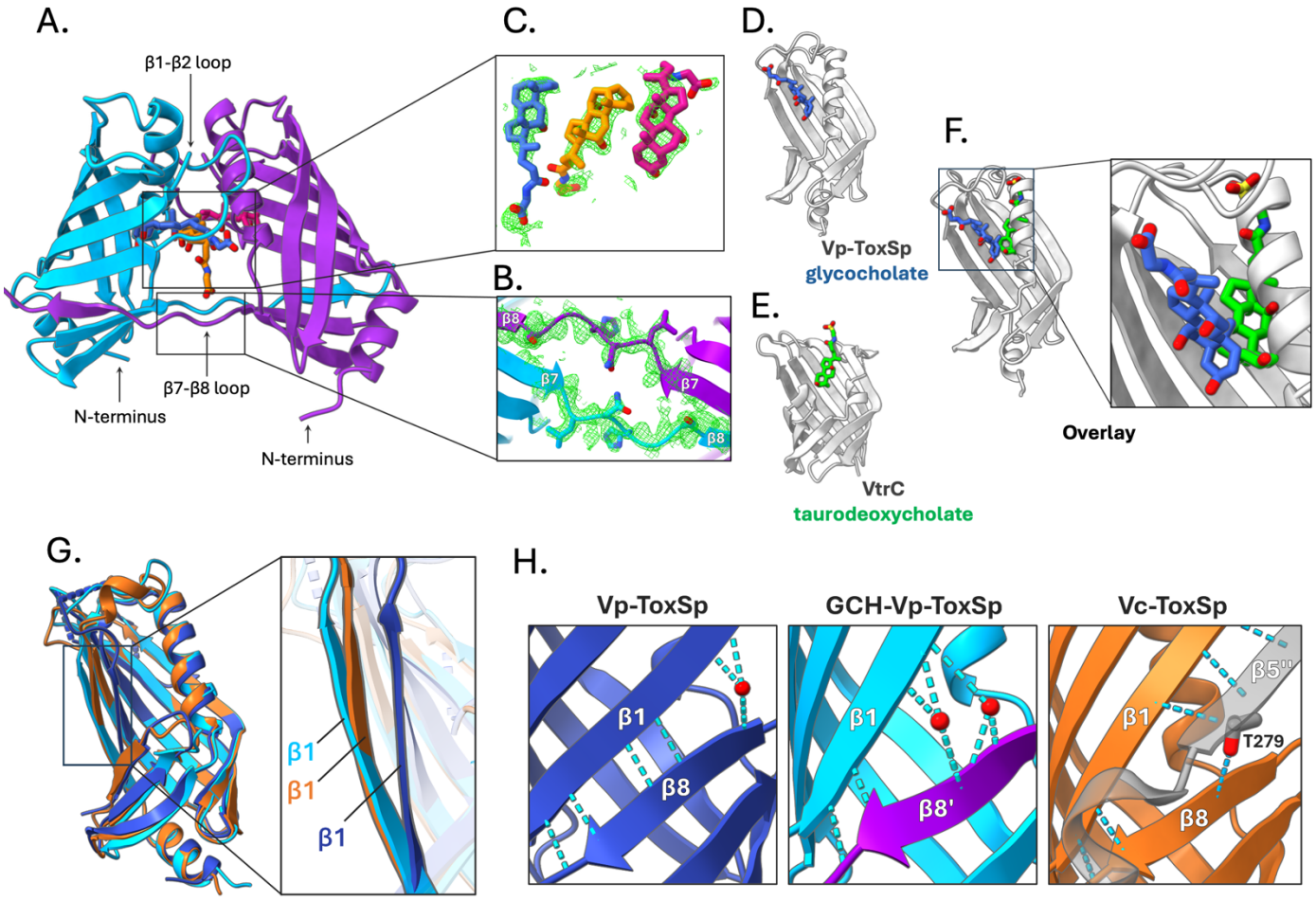

606
607

Figure 4

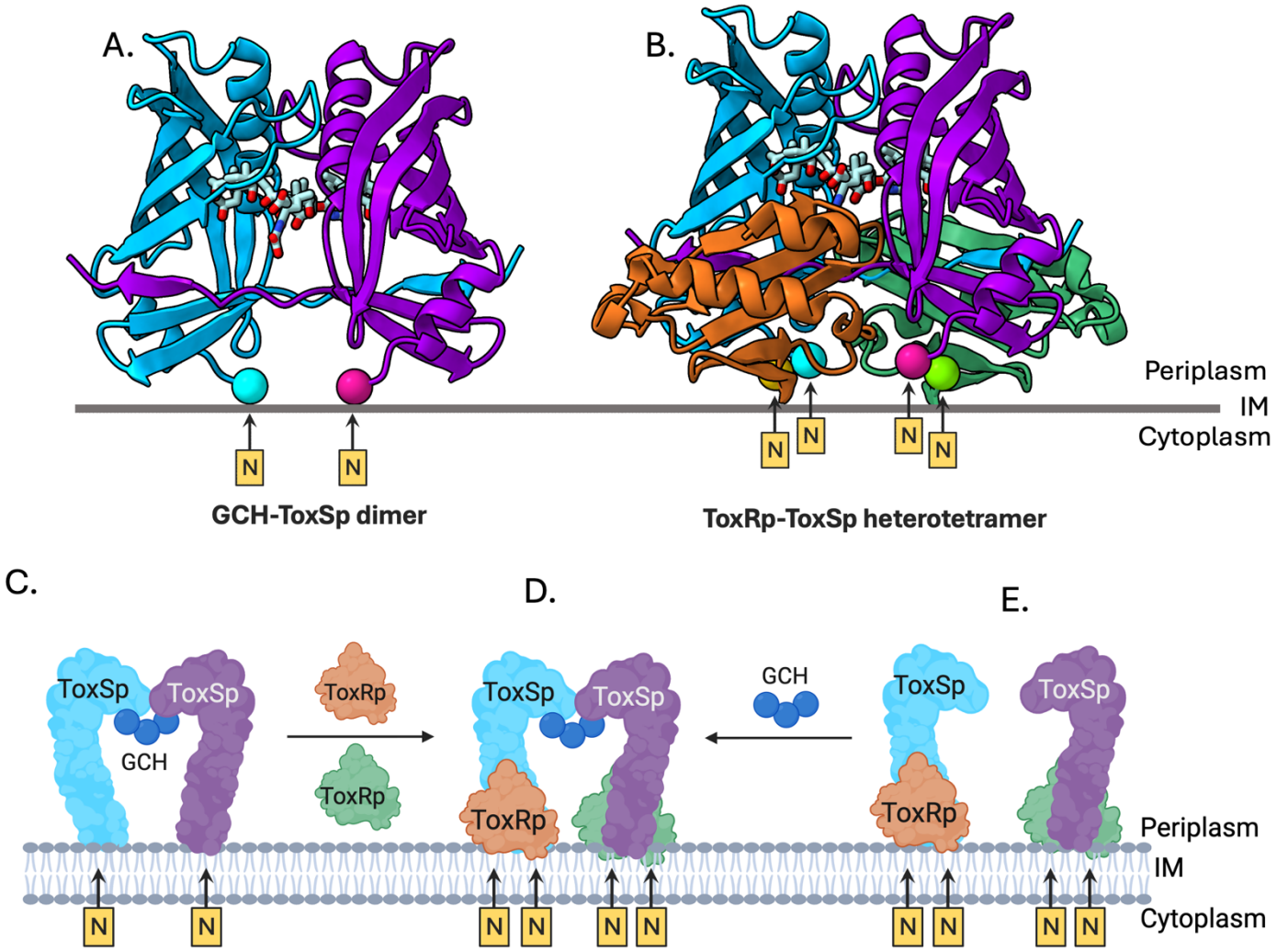
A.
B.
Periplasm
IM
Cytoplasm
N
GCH-ToxSp dimer
ToxRp-ToxSp heterotetramer
C.
D.
E.
ToxSp
GCH
ToxRp
Periplasm
IM
Cytoplasm

608